

# Green Synthesis of Titanium Oxide Nanoparticles Using *Murraya Paniculata* Leaf Extract for Enhanced Photocatalytic Degradation of Congo Red

Zalihat Abdullahi\*, Chukwuebuka Odinakachukwu Nweke, Abdulmumin Sumaila, Gideon Philip Azaki,

-Received: 12 March 2026/Accepted: 12 April 2026 /Published: 20 April 2026

<https://dx.doi.org/10.4314/cps.v13i4.8>

**Abstract:** Due to the growing amount of dye-laden industrial effluents being released into water bodies, there is a need for developing efficient and sustainable remediation methods. Herein, titanium oxide (TiO<sub>2</sub>) nanoparticles was synthesis via green route using the leaf extract from *Murraya paniculata* as reduction and capping/stabilizing agent. The biosynthesized titanium oxide nanoparticles were characterized using advance analytical tools such as X-ray diffraction (XRD), Fourier transform infrared spectroscopy (FTIR), Brunauer-Emmett-Teller (BET) and UV-visible (UV-Vis) spectrophotometry. XRD analysis confirmed the formation of highly crystalline anatase phase TiO<sub>2</sub> having crystallite size 18.4 nm while FTIR confirm the presence of Ti–O–Ti stretching mode. BET analysis revealed the presence of mesoporosity and a large specific surface area of 235.505 m<sup>2</sup>/g suitable for photocatalytic application. UV-visible revealed strong absorption of 256 nm in the UV region consistent with the optical properties of TiO<sub>2</sub> and suitable for photocatalytic processes. Nanoparticles showed 73.0% degradation efficiency of Congo red dye after 120 minute of irradiation with UV light.

**Keywords:** Green synthesis; TiO<sub>2</sub> nanoparticles; *Murraya paniculata*; photocatalytic degradation; Congo red dye; wastewater treatment

**Zalihat Abdullahi**

Department of Chemistry, Federal University of Technology, Minna, Niger State, Nigeria

Email: [z.abdullahi@futminna.edu.ng](mailto:z.abdullahi@futminna.edu.ng)

<https://orcid.org/0009-0009-3946-2951>

**Chukwuebuka Odinakachukwu Nweke**

Department of Chemistry, Federal University of Technology, Minna, Niger State, Nigeria

Email: [callmeebuka@outlook.com](mailto:callmeebuka@outlook.com)

**Abdumumin Sumaila**

Department of Chemistry, Confluence University of Science and Technology, Osara, Kogi State, Nigeria

Email: [sumailaa@custech.edu.ng](mailto:sumailaa@custech.edu.ng)

**Gideon Philip Azaki**

Department of Chemistry, Federal University of Technology, Minna, Niger State, Nigeria

Email: [azakigideon@gmail.com](mailto:azakigideon@gmail.com)

## 1.0 Introduction

Today, water contamination is one of the most urgent global environmental issues arising from rapid growth of industries and global populations (Turcu *et al.*, 2023). Diverse sectors, including but not limited to textiles, tanneries, pharmaceuticals, mining and cosmetics, produce enormous volumes of wastewater containing hazardous materials like heavy metals, organic toxins, industrial chemicals and synthetic dyes (Sangamnere *et al.*, 2023; Gupta and Mukhopadhyay, 2025). When these pollutants are released into waterways due to inadequate treatment of wastewater before discharge, they build up in aquatic environments and cause severe threats to both aquatic ecosystems and human life (Maheshwari *et al.*, 2021). Given that water is essential for all living organisms, deterioration in water quality poses serious risks to ecosystems and public health worldwide (Abdurahman *et al.*, 2021). An example of one type of pollutant that is of concern in industrial

wastewater comes from the synthetic dyes used by many sectors, such as textile, leather, paper and printing and plastic industries. Dye pollutants in water bodies significantly hinder penetration of sunlight into deeper regions of the aquatic environment, thereby decreasing light availability for photosynthetic activity (Al-Tohamy *et al.*, 2022)

There are currently over 100,000 varieties of synthetic dyes globally, with nearly 700,000 tons being produced annually across the various industries (Wu *et al.*, 2025). Due to inefficiencies during manufacturing and application of dyes, about 15 % of this amount enters into available freshwater systems which has an adverse impact on ecosystems (Yang *et al.*, 2022). However, manufacturers formulate synthetic dye products so they are extremely stable, thereby making them very persistent within the environments where they exist (Zeng *et al.*, 2021). Furthermore, dye pollutants reduce light penetration in aquatic systems, thereby inhibiting photosynthesis and disrupting the ecological balance of aquatic environments (Liu *et al.*, 2024).

Also, the presence of these pollutants in flowing waters reduces the ability of light to penetrate and adequately support the growth of algae that provide essential energy through the process of photosynthesis for the aquatic organism and also introduce toxic, mutagenic or even carcinogenic effects to all organism in the aquatic environment (Palma Soto *et al.*, 2024).

Congo red is a diazo dye characterized by a complex aromatic structure, which makes it highly stable and resistant to biodegradation. Due to its toxicity, it has been reported to exhibit carcinogenic, mutagenic, and adverse effects on the skin, eyes, respiratory, and reproductive systems.

Various techniques have been developed for the removal of dyes from wastewater which include adsorption (Liu *et al.*, 2022), flocculation/coagulation (Zhang *et al.*, 2020),

precipitation (Kumar & Lee, 2021) and reverse osmosis (Hassan *et al.*, 2022).

Despite their widespread application, these methods often suffer from limitations such as high operational costs, incomplete degradation, and the generation of secondary pollutants, highlighting the need for more efficient and sustainable treatment approaches.

In addition, several of these methods remove dyes primarily through adsorption, meaning the pollutants remain in the environment in potentially toxic forms, consequently, attention has shifted toward the use of low-cost adsorbents and procedures for wastewater treatment.

Photocatalysis has emerged as an effective and environmentally friendly technique for wastewater treatment, as it enables the complete mineralization of organic pollutants into harmless end products such as CO<sub>2</sub> and water. Semiconductor photocatalysts such as TiO<sub>2</sub> generate reactive oxygen species (ROS) under UV irradiation, which play a crucial role in the degradation of organic contaminants.

Conventional methods for nanoparticle synthesis, such as sol-gel, chemical vapor deposition, hydrothermal treatment, and precipitation techniques, generally require high energy input and the use of toxic chemicals as stabilizing and capping agents (Al Ja'farawy *et al.*, 2022). Green synthesis approaches, which utilize biological systems such as plant extracts, offer a sustainable and eco-friendly alternative for nanoparticle production. Many of the phytochemicals, such as flavonoids and phenols, found in plants extract can reduce and stabilize nanoparticles, resulting in non-toxic, biocompatible nanoparticles (Malkari-Katika & Boddu, 2025). "However, despite the growing interest in green synthesis of TiO<sub>2</sub> nanoparticles, there is limited research on the use of *Murraya paniculata* leaf extract as a reducing and stabilizing agent. Furthermore, its effectiveness in enhancing photocatalytic degradation of Congo red dye



has not been extensively explored. Despite the extensive application of TiO<sub>2</sub> nanoparticles in photocatalysis, most synthesis methods rely on chemical routes that are costly and environmentally hazardous. Although green synthesis using plant extracts has gained attention, there is limited information on the use of *Murraya paniculata* for the synthesis of TiO<sub>2</sub> nanoparticles and its effectiveness in degrading Congo red dye. Therefore, this study aims to synthesize TiO<sub>2</sub> nanoparticles using *Murraya paniculata* leaf extract as a reducing and stabilizing agent, characterize the synthesized nanoparticles, and evaluate their photocatalytic efficiency for Congo red degradation. This study provides a cost-effective, environmentally friendly, and sustainable approach for wastewater treatment, contributing to the development of green nanotechnology for environmental remediation.

## 2.0 Materials and Methods

### 2.1 Reagents and Chemicals

Titanium tetra-isopropoxide, Ti(OCH(CH<sub>3</sub>)<sub>2</sub>)<sub>4</sub> (98%), was purchased from Merck, USA. Absolute ethanol (98%) was obtained from BDH Chemicals, England, while Congo red dye was procured from Loba Chemie, India. Distilled water was obtained from the university laboratory. All reagents were of analytical grade and used without further purification.

### 2.2 Plant Material Collection and Preparation of Extract

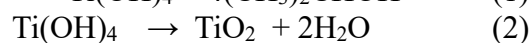
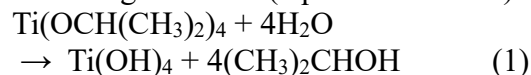
Fresh leaves of *Murraya paniculata* were collected from the premises of the Federal University of Technology, Minna, Nigeria. The leaves were thoroughly washed with tap water followed by distilled water to get rid of dust and other surface contaminants prior to being chopped into small pieces. To extract bioactive compounds, 50 g of the chopped leaves were added to a 1 L beaker containing 250 cm<sup>3</sup> of distilled water and then heated to 80 °C for 20

minutes. After cooling, the extract was filtered using Whatman filter paper No. 1 and the clear filtrate was used immediately as a stabilizing/capping and reducing agent for the synthesis of TiO<sub>2</sub> nanoparticles. This method helps preserve active phytochemicals, which enhances nanoparticle stability, improves nucleation efficiency, and ensures better reproducibility during synthesis.

### 2.3 Green Synthesis of TiO<sub>2</sub> Nanoparticles

A volume of 60 cm<sup>3</sup> of *Murraya paniculata* leaf extract was added dropwise to 20 cm<sup>3</sup> of 0.5 mol/dm<sup>3</sup> titanium tetra-isopropoxide solution, followed by the addition of 60 cm<sup>3</sup> of ethanol under continuous stirring at a temperature of 50 °C for 3 hours to ensure effective interaction between plant phytochemicals and titanium oxide precursor. Stirring was continued until a visible colour change was noticed indicating the formation of nanoparticles. The product was left to settle and the supernatant was decanted while the precipitate was washed with ethanol followed by distilled water until a neutral pH was obtained. The precipitate was dried in an oven at 100 °C and subsequently calcined at 450 °C for 3 hours in a muffle furnace to enhance crystallinity, remove residual organic matter, and obtain phase-pure TiO<sub>2</sub> nanoparticles (Kaushal *et al.*, 2025).

The formation of TiO<sub>2</sub> nanoparticles via the green synthesis route can be represented by the following reactions (equations 1 and 2)



### 2.4 Characterization of TiO<sub>2</sub> Nanoparticles

The synthesized TiO<sub>2</sub> nanoparticles were characterized using various analytical techniques to determine their optical properties, functional groups, crystallinity, phase composition, and surface area, all of which influence photocatalytic performance.



Fourier Transform Infrared (FTIR) spectroscopy was used to determine the surface functional groups present and to confirm that phytochemicals from *Murraya paniculata* extract contributed to the formation of the nanoparticles. The FTIR spectra were recorded

in the range of 500–4000  $\text{cm}^{-1}$  using an Alpha II spectrometer (Bruker). X-ray diffraction (XRD) analysis was carried out using an XPERT-3 PXRD instrument with  $\text{CuK}\alpha$  radiation ( $\lambda = 1.54 \text{ \AA}$ ) over a  $2\theta$  range of  $10^\circ$ – $80^\circ$ .



**Plate I: *Murraya paniculata* Leaves**

The double-beam UV-Vis spectrophotometer (Shimadzu UV-2600, Shimadzu Corporation, Kyoto, Japan) was used for this work using a 1.0 cm quartz cuvette at room temperature in ambient lab conditions. To ensure the samples were not saturated and therefore result in inaccurate spectral readings, deionized water was used to prepare sample dilutions. The UV-Vis absorption data were collected over spectral range of 200 - 800 nm at a scan rate of 400 nm/min and a bandwidth of 1.0 nm (Kumar *et al.*, 2023). Surface area analysis was performed using the Brunauer–Emmett–Teller (BET) method on a Quantachrome Autosorb-iQ surface area analyzer.

### **2.5 Preparation of Congo Red Dye Stock Solution**

A stock solution of Congo red (1000 ppm) was prepared by dissolving 0.5 g of the dye in 500  $\text{cm}^3$  of distilled water in a 1000 mL beaker under continuous stirring until complete dissolution. Serial dilution was then performed to obtain the required working concentrations.

### **2.6 Photocatalytic Degradation of Congo Red Dye**

Congo red dye was used as a model organic pollutant to evaluate the photocatalytic activity of the green-synthesized  $\text{TiO}_2$  nanoparticles. A known weight (0.2 g) of  $\text{TiO}_2$  nanoparticles were added to 500  $\text{cm}^3$  of a stock solution of Congo Red (10 mg/L) that had been made in distilled water. The suspension was stirred in the dark for 30 minutes to establish adsorption–desorption equilibrium between the dye molecules and the catalyst surface. The mixture



was stirred for approximately half an hour in the dark using a magnetic stirrer. After equilibration, the suspension was irradiated using a 250 W mercury lamp.

At 30-minute intervals, 5 cm<sup>3</sup> aliquots were withdrawn, centrifuged, and the supernatant was analyzed using a UV-Vis spectrophotometer at 497 nm, corresponding to the maximum absorption wavelength ( $\lambda_{\text{max}}$ ) of Congo red (Narayanaswamy & Ward, 2021; Landge *et al.*, 2022). The extent of dye degradation was calculated using equation 3

$$\text{Degradation (\%)} = \frac{A_0 - A_t}{A_0} \times 100 \quad (3)$$

where  $A_0$  = absorbance after adsorption equilibrium and  $A_t$  = absorbance at time  $t$ .

### 3.0 Results and Discussion

#### 3.1 XRD analysis of TiO<sub>2</sub> nanoparticles

The XRD analysis carried out on TiO<sub>2</sub> nanoparticles is represented by the spectra

shown in Fig. 1. The X-ray diffraction (XRD) pattern of the green-synthesized titanium dioxide (TiO<sub>2</sub>) nanoparticles provides clear insight into their crystalline structure, phase composition, and overall quality. The diffraction profile displays a series of sharp and well-defined peaks across the 2 $\theta$  range of 10° to 80°, indicating that the synthesized nanomaterial possesses a high degree of crystallinity.

The prominent diffraction peaks observed at approximately 25.3°, 37.8°, 48.0°, 54.0°, 56.0°, and 62.7° are indexed to the crystallographic planes (101), (004), (200), (105), (211), and (204), respectively. These reflections are characteristic of the anatase phase of TiO<sub>2</sub> and are in excellent agreement with the standard reference pattern (JCPDS Card No. 21-1272). The strong intensity of the (101) peak at around 25.3° further confirms that anatase is the dominant crystalline phase in the sample.

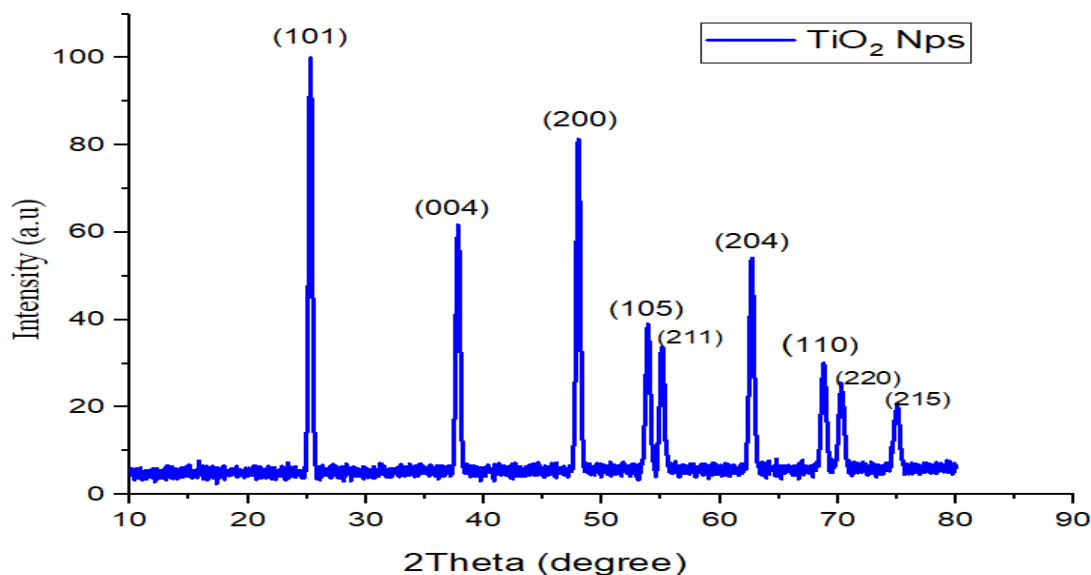


**Fig. 1: XRD Pattern of TiO<sub>2</sub> Nanoparticles**

Importantly, no additional diffraction peaks corresponding to other polymorphs such as rutile or brookite are detected in the pattern. This absence of secondary phase peaks indicates that the synthesized nanoparticles are phase-pure and that the green synthesis route

employed is effective in selectively producing the anatase structure. The narrow peak widths and high intensities also suggest that the nanoparticles are well crystallized, with minimal structural defects.



The consistency of these findings with previously reported studies on plant-mediated synthesis of TiO<sub>2</sub> nanoparticles further validates the reliability of the method used. Similar diffraction patterns have been documented in the literature, confirming that green synthesis approaches typically favor the formation of pure anatase TiO<sub>2</sub>.

From an application standpoint, the predominance of the anatase phase is highly advantageous, particularly for catalytic and photocatalytic processes. Anatase TiO<sub>2</sub> is known for its relatively high surface area, which provides more active sites for reactions, as well as its superior charge separation efficiency, which reduces electron-hole recombination. These properties collectively enhance its effectiveness in applications such

as pollutant degradation and environmental remediation.

The crystallite size, which provides information about the nanoscale structural characteristics was calculated using the Debye-Scherrer equation and was found to be 18.4 nm (Yang *et al.*, 2022).

$$D = \frac{K\lambda}{\beta \cos\theta} \quad (4)$$

where D is the average crystallite size (in nm), K is the Scherrer constant (typically 0.9),  $\lambda$  is the X-ray wavelength (1.5406 Å),  $\beta$  is the full width at half maximum of the most intense diffraction peak (in radians) and  $\theta$  is the Bragg's angle (in degrees).

### 3.2 FTIR Analysis of TiO<sub>2</sub> Nanoparticles

Fig. 2 represents the FTIR spectra of the green synthesized titanium oxide nanoparticles

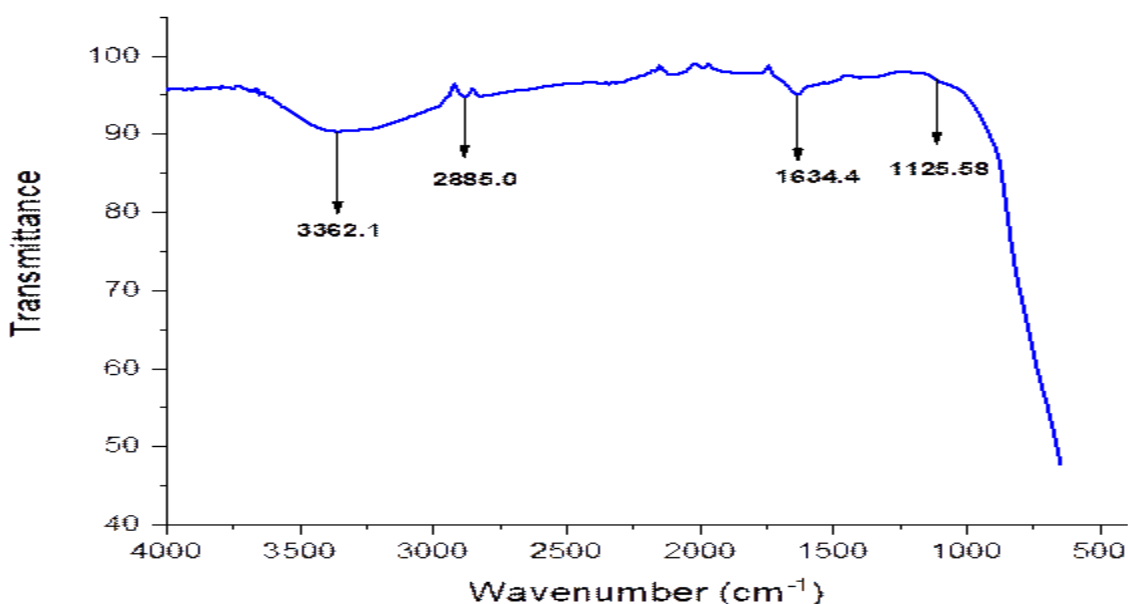


**Fig. 2: FTIR Spectra of TiO<sub>2</sub> Nanoparticles**

The FTIR spectrum of the green-synthesised TiO<sub>2</sub> nanoparticles shown in Fig. 2 displays the FTIR spectrum of the TiO<sub>2</sub> nanoparticles. The broad absorption band observed at 3200–3500 cm<sup>-1</sup> is attributed to O–H stretching vibrations, indicating the presence of surface hydroxyl groups, which play a significant role in

photocatalytic reactions. This observation is consistent with reports by Koppala *et al.* (2021), which highlight the role of hydroxyl groups in enhancing surface reactivity of plant-mediated nanoparticles. The absorption band at 2885 cm<sup>-1</sup> is attributed to C–H stretching vibrations associated with organic compounds



such as phenolics, flavonoids, and other biomolecules present in the plant extract. These biomolecules act as reducing and stabilizing agents during nanoparticle synthesis. Functional groups such as  $-OH$  and  $-NH$  present in these biomolecules contribute to the reduction of  $Ti^{4+}$  ions and stabilization of the synthesized nanoparticles, thereby preventing agglomeration.

The band observed at  $1600-1650\text{ cm}^{-1}$  is assigned to  $C=O$  stretching vibrations. Similar observations have been reported for plant-mediated  $TiO_2$  nanoparticles synthesized using *Azadirachta indica* and *Camellia sinensis*, where phytochemicals contribute to nanoparticle stabilization (Quintanilla-Villanueva *et al.*, 2025). These residual organic species may also enhance photocatalytic activity by acting as photosensitizers. The absorption band observed around  $1125\text{ cm}^{-1}$  is associated with  $Ti-O-Ti$  stretching vibrations, indicating the formation of  $TiO_2$  nanoparticles. All observed peaks are consistent with previous reports on green-synthesized  $TiO_2$  nanoparticles.

### 3.3 Brunauer-Emmett-Teller (BET) Analysis of the Synthesized $TiO_2$ Nanoparticles

Table 1 summarizes the BET analysis of the synthesized  $TiO_2$  nanoparticles. The specific surface area was determined using the BET method, while the pore size and pore volume were obtained from Barrett-Joyner-Halenda (BJH) plots. The specific surface area was found to be  $235.505\text{ m}^2/\text{g}$ , indicating a large number of active sites available for photocatalytic activity. The average pore diameter was  $2.128\text{ nm}$ , suggesting a mesoporous structure in accordance with IUPAC classification ( $2-50\text{ nm}$ ) (Deliza *et al.*, 2025). Furthermore, the pore volume of  $0.132\text{ cm}^3/\text{g}$  confirms the presence of a well-developed porous network, which enhances the textural properties of the nanoparticles, likely due to the influence of plant-derived phytochemicals during synthesis.

**Table 1: Summary of BET Analysis**

S/N	Parameter	Value
1	Surface area	$235.505\text{ m}^2/\text{g}$
2	Pore size	$2.128\text{ nm}$
3	Pore volume	$0.132\text{ cm}^3/\text{g}$

### 3.4 UV-Visible Spectroscopic Analysis of $TiO_2$

Fig. 3 shows the UV-vis spectra of the green synthesized  $TiO_2$  nanoparticles

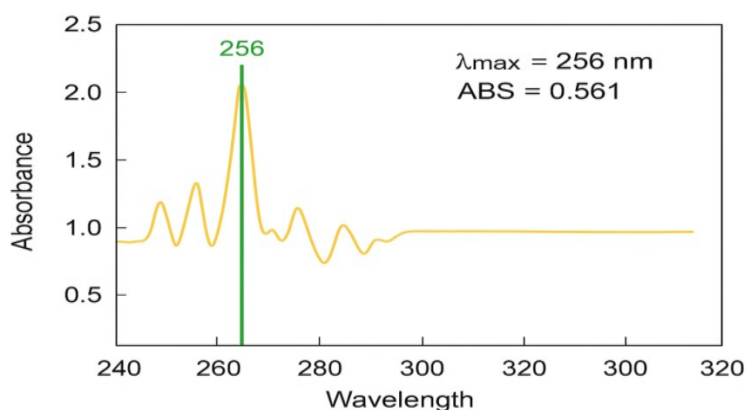


**Fig. 3: UV-Visible Spectrophotometer Absorption Graph**

From Fig. 3, A distinct absorption peak is observed at  $256\text{ nm}$  with an absorbance of

$0.561$ , located in the ultraviolet region of the spectrum. This peak corresponds to the



characteristic electronic transition in  $\text{TiO}_2$ , attributed to charge transfer from the valence band (O 2p) to the conduction band (Ti 3d). The observed absorption at 256 nm indicates a blue shift relative to bulk  $\text{TiO}_2$ , which is commonly associated with reduced particle size and quantum confinement effects. Similar findings were reported by Saini & Kumar (2023), who observed absorption maxima between 250 and 280 nm for plant-mediated  $\text{TiO}_2$  nanoparticles and the optical stability of  $\text{TiO}_2$  nanoparticles synthesized utilizing plant extracts. This suggests that phytochemical constituents of the plant extract effectively

facilitated the reduction and stabilization of Ti species during synthesis, contributing to the observed optical properties.

### 3.5 Photocatalytic Degradation of Congo Red Dye

Figs 4 and 5 show a progressive decrease in absorbance with increasing irradiation time, indicating the degradation of Congo red dye in the presence of the photocatalyst. This reduction in absorbance confirms the photocatalytic efficiency of the green-synthesized  $\text{TiO}_2$  nanoparticles.

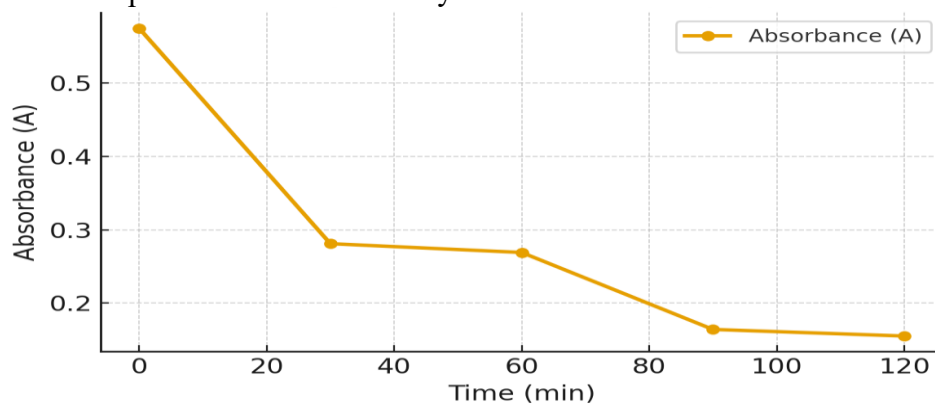


**Fig. 4: Variation of Absorbance with Respect to Time for the Photocatalytic Degradation of Congo Red Dye Under UV Irradiation Using Green-Synthesised  $\text{TiO}_2$  Nanoparticles**

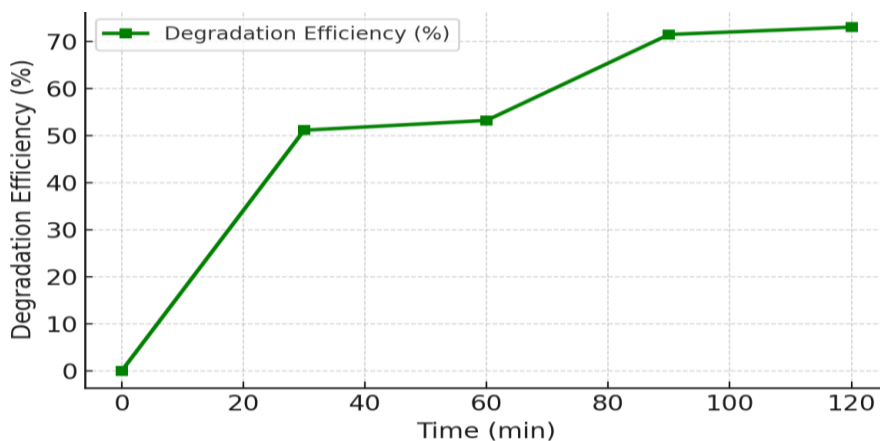


**Fig. 5: Photocatalytic Degradation Efficiency of  $\text{TiO}_2$  Nanoparticles with Respect to Time**

From Fig 4 and 5, the absorbance values decreased progressively with increase in irradiation time, signifying the breakdown of

dye molecules in the presence of the photocatalyst. The absorbance and degradation efficiency is shown in Figs 4 and 5. The



observed reduction in absorbance intensity with increase in time indicate the progressive degradation of Congo Red, confirming the photocatalytic efficiency of the green-synthesised TiO<sub>2</sub> nanoparticles attributable to the synergy of the high surface area, nanocrystalline structure and presence of surface hydroxyl moieties as evident in the characterization results. The absorbance decreased from an initial value of 0.575 to 0.155 over 120 minutes of irradiation, corresponding to a maximum degradation efficiency of 73%. Under UV irradiation, TiO<sub>2</sub> generates electron-hole pairs, which react with water and dissolved oxygen to produce reactive oxygen species (ROS) such as hydroxyl radicals ( $\bullet\text{OH}$ ) and superoxide radicals ( $\text{O}_2\bullet^-$ ). These reactive species attack the azo bonds ( $-\text{N}=\text{N}-$ ) and aromatic structures of Congo red, leading to its degradation into less harmful products.

A plateau in degradation efficiency at longer irradiation times may be attributed to a reduced reaction rate due to the decreased concentration of the dye.

#### 4.0 Conclusion

The present study successfully demonstrated the green synthesis of titanium dioxide (TiO<sub>2</sub>) nanoparticles using *Murraya paniculata* leaf extract as a sustainable and environmentally friendly approach. The plant extract effectively served as both a reducing and stabilizing agent, enabling nanoparticle formation without the use of hazardous chemicals associated with conventional synthesis methods.

Comprehensive characterization confirmed the successful synthesis of TiO<sub>2</sub> nanoparticles. FTIR analysis revealed the presence of Ti-O-Ti functional groups, while XRD results indicated a predominantly anatase phase with good crystallinity and phase purity. BET analysis showed a high specific surface area (235.505 m<sup>2</sup>/g) and a mesoporous structure, as supported by the pore size and pore volume

results. Furthermore, UV-Vis spectroscopy demonstrated strong absorption in the ultraviolet region, consistent with the expected optical properties of TiO<sub>2</sub> and its suitability for photocatalytic applications.

The photocatalytic activity of the synthesized nanoparticles was evaluated using Congo red dye as a model pollutant. The TiO<sub>2</sub> nanoparticles achieved a degradation efficiency of 73.0% within 120 minutes under UV irradiation. This performance can be attributed to the high surface area, nanoscale crystallinity, and the presence of surface hydroxyl groups, which enhance the generation of reactive species during photocatalysis.

Although the degradation efficiency is slightly lower than that reported for doped or composite TiO<sub>2</sub> systems, the present approach offers a simple, cost-effective, and environmentally benign alternative. Overall, the findings indicate that *Murraya paniculata*-mediated TiO<sub>2</sub> nanoparticles possess significant potential for application in sustainable wastewater treatment and environmental remediation.

#### 5.0 References

- Abdurahman, M. H., Abdullah, A. Z., & Shoparwe, N. F. (2021). A comprehensive review on sonocatalytic, photocatalytic, and sonophotocatalytic processes for the degradation of antibiotics in water: Synergistic mechanism and degradation pathway. *Chemical Engineering Journal*, 413, 127412, <https://doi.org/10.1016/j.cej.2020.127412>
- Al Ja'farawy, M. S., Purwanto, A., & Widiyandari, H. (2022). Carbon quantum dots supported zinc oxide (ZnO/CQDs) efficient photocatalyst for organic pollutant degradation—A systematic review. *Environmental Nanotechnology, Monitoring & Management*, 18, 100681, <https://doi.org/10.1016/j.enmm.2022.100681> [Get rights and content](#)



- Al-Tohamy, R., Ali, S. S., Li, F., Okasha, K. M., Mahmoud, Y. A. G., Elsamahy, T., & Sun, J. (2022). A critical review on the treatment of dye-containing wastewater: Ecotoxicological and health concerns of textile dyes and possible remediation approaches for environmental safety. *Ecotoxicology and Environmental Safety*, 231, 113160, <https://doi.org/10.1016/j.ecoenv.2021.113160>[Get rights and content](#)
- Basu, H., Saha, S., Pimple, M. V., & Singhal, R. K. (2019). Novel hybrid material humic acid impregnated magnetic chitosan nanoparticles for decontamination of uranium from aquatic environment. *Journal of Environmental Chemical Engineering*, 7, 3, 103110. <https://doi.org/10.1016/j.jece.2019.103110>
- Deliza, D., Safni, S., Zein, R., & Putri, R. A. (2025). Novel green synthesis of titanium oxide using *Lansium domesticum* Correa for photocatalytic degradation of methyl orange. *Journal of Ecological Engineering*, 26, 8, pp. 1–10, <https://doi.org/10.12911/22998993/203528>
- Gupta, B. G., & Mukhopadhyay, R. (2025). Heavy metal contamination from textile wastewater and its health impacts: A case study from West Bengal with sustainable remediation approaches. *Scientific Reports*, 15, 1, 29578, <https://doi.org/10.1038/s41598-025-13357-w>
- Hassan, A. A., Elwardany, A. E., Ookawara, S., Sekiguchi, H., & Hassan, H. (2022). Performance and economic analysis of hybrid solar collectors-powered integrated adsorption/reverse osmosis multigeneration system. *International Journal of Energy Research*, 46, 14, pp. 19414–19437, <https://doi.org/10.1002/er.8512>
- Kaushal, S., Thakur, N., & Kumar, K. (2025). Green synthesis of cerium co-doped Ba and Zn/TiO<sub>2</sub> nanoparticles: Photocatalytic degradation of Congo red and rhodamine B. *International Journal of Environmental Analytical Chemistry*, 105, 20, pp. 9079–9101, <https://doi.org/10.1080/03067319.2025.2494062>
- Koppala, S., Balan, R., Banerjee, I., Li, K., Xu, L., Liu, H., Kumar, D. K., Raghava Reddy, K., & Sadhu, V. (2021). Room temperature synthesis of novel worm-like tin oxide nanoparticles for photocatalytic degradation of organic pollutants. *Materials Science for Energy Technologies*, 4, pp. 113–118. <https://doi.org/10.1016/j.mset.2021.03.002>
- Kumar, M., Ambika, S., Hassani, A., & Nidheesh, P. V. (2023). Waste to catalyst: Role of agricultural waste in water and wastewater treatment. *Science of the Total Environment*, 858, 159762. <https://doi.org/10.1016/j.scitotenv.2022.159762>
- Kuyucu, A. E., Selçuk, A., Önal, Y., Alacabey, İ., & Erol, K. (2025). Effective removal of dyes from aqueous systems by waste-derived carbon adsorbent: Physicochemical characterization and adsorption studies. *Scientific Reports*, 15, 1, 28835, <https://doi.org/10.1038/s41598-025-13685-x>
- Landge, V. K., Huang, C.-M., Hakke, V. S., Sonawane, S. H., Manickam, S., & Hsieh, M.-C. (2022). Solar-energy-driven Cu-ZnO/TiO<sub>2</sub> nanocomposite photocatalyst for the rapid degradation of Congo red azo dye. *Catalysts*, 12, 6, 605, <https://doi.org/10.3390/catal12060605>
- Liu, Y., Chen, J., Duan, D., Zhang, Z., Liu, C., Cai, W., & Zhao, Z. (2024). Environmental impacts and biological technologies toward sustainable treatment of textile dyeing wastewater: A review. *Sustainability*, 16, 24, 10867, <https://doi.org/10.3390/su162410867>



- Liu, Z., Zhang, W., Zhao, X., Sheng, X., Hu, Z., Wang, Q., & Wang, X. (2022). Efficient adsorption-assisted photocatalysis degradation of Congo red through loading ZIF-8 on KI-doped TiO<sub>2</sub>. *Materials*, 15, 8, 2857, <https://doi.org/10.3390/ma15082857>
- Ljubas, D., Vučemilović, A., Briševac, D., Cajner, H., & Juretić, H. (2025). Optimized solar-simulated photocatalysis of Congo red dye using TiO<sub>2</sub>: Toward a sustainable water treatment approach. *Molecules*, 30, 11, 2388, <https://doi.org/10.3390/molecules30112388>
- Malkari-Katika, R., & Boddu, S. (2025). Advanced photocatalysis with biochar-TiO<sub>2</sub> composite for efficient oxidation of Congo red dye. *Environmental Monitoring and Assessment*, 197, 7831, <https://doi.org/10.1007/s10661-025-14290-1>
- Narayanaswamy, N., & Ward, C. A. (2021). Specific surface area of nanopowders from argon adsorption at 77 and 87 K: Zeta adsorption isotherm approach. *The Journal of Physical Chemistry C*, 125, 51, pp. 28115–28131, <https://doi.org/10.1021/acs.jpcc.1c08945>
- Ogunsakin, R. E., Olugbara, O. O., Moyo, S., & Israel, C. (2021). Meta-analysis of studies on depression prevalence among diabetes mellitus patients in Africa. *Heliyon*, 7, 5, pp. e07085 <https://doi.org/10.1016/j.heliyon.2021.e07085>
- Palma Soto, E., Rodríguez González, C. A., Luque Morales, P. A., Reyes Blas, H., & Carrillo Castillo, A. (2024). Degradation of organic dye Congo red by heterogeneous solar photocatalysis with Bi<sub>2</sub>S<sub>3</sub>, Bi<sub>2</sub>S<sub>3</sub>/TiO<sub>2</sub>, and Bi<sub>2</sub>S<sub>3</sub>/ZnO thin films. *Catalysts*, 14, 9, 589, <https://doi.org/10.3390/catal14090589>
- Quintanilla-Villanueva, G. E., Sicardi-Segade, A., Luna-Moreno, D., Núñez-Salas, R. E., Villarreal-Chiu, J. F., & Rodríguez-Delgado, M. M. (2025). Recent advances in Congo red degradation by TiO<sub>2</sub>-based photocatalysts under visible light. *Catalysts*, 15, 1, 84, <https://doi.org/10.3390/catal15010084>
- Saini, R., & Kumar, P. (2023). Green synthesis of TiO<sub>2</sub> nanoparticles using *Tinospora cordifolia* plant extract and its potential application for photocatalysis and antibacterial activity. *Inorganic Chemistry Communications*, 156, 111221, <https://doi.org/10.1016/j.inoche.2023.111221>
- Sangamnere, R., Misra, T., Bherwani, H., Kapley, A., & Kumar, R. (2023). A critical review of conventional and emerging wastewater treatment technologies. *Sustainable Water Resources Management*, 9, 2, 58, <https://doi.org/10.1007/s40899-023-00829-y>
- Siddiqui, S. I., Allehyani, E. S., Al-Harbi, S. A., Hasan, Z., Abomuti, M. A., Rajor, H. K., & Oh, S. (2023). Investigation of Congo red toxicity towards different living organisms: A review. *Processes*, 11, 3, 807, <https://doi.org/10.3390/pr11030807>
- Turcu, E., Coromelci, C. G., Harabagiu, V., & Ignat, M. (2023). Enhancing the photocatalytic activity of TiO<sub>2</sub> for the degradation of Congo red dye by adjusting the ultrasonication regime applied in its synthesis procedure. *Catalysts*, 13, 2, 345, <https://doi.org/10.3390/catal13020345>
- Wu, J., Sun, X., Zhu, K., Wang, Q., Tang, J., Wang, Q., Guo, J., & Khor, S. M. (2025). A stable and regenerative TiO<sub>2</sub>/Bi<sub>2</sub>MoO<sub>6</sub> photocatalyst for highly effective degradation of rhodamine B and Congo red. *International Journal of Environmental Analytical Chemistry*, 105, 16, pp. 4688–4706, <https://doi.org/10.1080/03067319.2024.2376901>
- Yang, Y., Liu, K., Sun, F., Liu, Y., & Chen, J. (2022). Enhanced performance of photocatalytic treatment of Congo red wastewater by CNTs-Ag-modified TiO<sub>2</sub>



under visible light. *Environmental Science and Pollution Research*, 29, 11, pp. 15516–15525, <https://doi.org/10.1007/s11356-021-16734-w>

- Zeng, Q., Wang, Y., Zan, F., Khanal, S. K., & Hao, T. (2021). Biogenic sulfide for azo dye decolorization from textile dyeing wastewater. *Chemosphere*, 283, pp. 131158, <https://doi.org/10.1016/j.chemosphere.2021.131158>
- Zhang, Y., Zhang, Q., Hou, D., & Zhang, J. (2020). Tuning interfacial structure and mechanical properties of graphene oxide sheets/polymer nanocomposites by controlling functional groups of polymer. *Applied Surface Science*, 504, 144152. <https://doi.org/10.1016/j.apsusc.2019.144152>

2

The publisher has the right to make the data public

#### **Conflict of Interest**

The authors declared no conflict of interest

#### **Ethical Considerations**

Not applicable

#### **Competing interest**

The authors report no conflict or competing interest

#### **Funding**

The author declared no source of funding

#### **Authors' Contributions**

Zaliha Abdullahi conceptualized and supervised the study, designed methodology, and reviewed the manuscript. Chukwuebuka Odinakachukwu Nweke conducted experiments, characterization, and drafted the manuscript. Abdulmumin Sumaila analyzed data and interpreted results. Gideon Philip Azaki assisted in sample preparation, data collection, and literature review. All authors revised and approved the final manuscript.

#### **Declaration**

#### **Consent for publication**

Not Applicable

#### **Availability of data and materials**

